

## Treatment Planning for Heavy-ion Radiotherapy: Biological Optimization of Multiple Beam Ports

MICHAEL KRÄMER\*

GSI Biophysik, Planck-Str. 1, D-64291 Darmstadt, Germany

*(Received, February 22, 2000)*

*(1st. Revision received, June 26, 2000)*

*(2nd. Revision received, September 11, 2000)*

*(Accepted, October 18, 2000)*

### **Radiotherapy/Carbon ion beams/Treatment planning/Biologically effective dose distribution/ Multiport irradiation**

A crucial task in radiotherapy is dose conformation to the prescribed target volume whilst sparing the surrounding healthy tissue around as much as possible. One of the best approaches so far is active dose shaping in three dimensions using scanned beams of charged particles, like carbon ions. Besides their inverse dose profile and minimal lateral scattering, carbon ions have the advantage that their RBEs increase towards the end of their range. An active beam-delivery system for intensity-modulated carbon-ion beams has been operational at GSI since December, 1997. In order to ensure dose conformation, inverse treatment planning with respect to the biologically effective dose distribution must be applied. A typical patient irradiation comprises two singly optimized opposing fields. This paper discusses the superposition of biologically effective dose distributions for radiotherapy with  $^{12}\text{C}$  ions, which is non-trivial due to the nonlinear nature of the dose response of biological systems. Sum rules for the nonlinear addition of singly optimized fields are derived. This method is being used clinically, and has been successfully applied to more than 50 patients.

### **INTRODUCTION**

Since December, 1997, a radiotherapy unit has been operational at Gesellschaft für Schwerionenforschung (GSI), Darmstadt (Germany), using beams of  $^{12}\text{C}$  ions to treat patients with head and neck tumours. An intensity-modulated magnetic raster scan device together with active energy variation of GSI's SIS synchrotron allows completely active dose shaping in three dimensions, resulting in a good tumour-conform dose delivery. Several thousands of narrow ion pencil beams with individual lateral positions, ion energies and particle fluences are combined to form an intensity-modulated field of high granularity. Beams of  $^{12}\text{C}$  ions are

---

\*Corresponding author: Phone; +49–6159–71–2157, Fax; +49–6159–712106, E-mail; M.Kraemer@gsi.de

high-LET radiation and show a large relative biological effectiveness (RBE) towards the end of their range, something which adds to the already favourable characteristics of ion beams.

Both, the physical and radiobiological properties of fast  $^{12}\text{C}$  ions are included in routine treatment planning with the code system TRiP (TReatment planning for Particles)<sup>1)</sup>. Due to the very high number of degrees of freedom, inverse planning must be applied to determine the various beam spot positions, energies and particle fluences in order to achieve the optimum dose distribution across the target volume. In practice, most patients are irradiated with two approximately opposing fields (beam ports) within a short period of time, i.e. usually less than one hour. In principle, this would require a simultaneous optimization of the overlapping heavy-ion fields. However, the inherent ambiguities of a biologically effective dose superposition within the same target voxel complicates the determination of the particle fluences. Hence, we decided — at least for the startup phase of the GSI radiotherapy project — to optimize each field separately (single beam port optimization). This approach has the advantage that calculations can be performed in a water-equivalent beams-eye-view system, which is easier than on the CT grid. After optimization, the single beam ports are overlaid to obtain the final biologically effective dose distributions on the CT grid. However, the biologically effective dose values add nonlinearly, and the RBE varies across the target volume. Therefore, it has to be shown that such a procedure nonetheless yields a reasonable dose distribution. Furthermore, prescriptions have to be worked out for selecting the partial dose levels, which then add up to the desired final dose.

The problem addressed here is very specific to high-LET radiation where RBE has to be incorporated<sup>2,3)</sup>. Various therapy sites use proton gantries and are routinely used to perform multiport treatment<sup>4)</sup>. However, for protons the RBE is usually assumed to have a constant value of 1.1 in clinical practice, which is definitely not appropriate for heavier ions. At present, only at NIRS<sup>5)</sup> patients are treated with large-RBE radiation ( $^{12}\text{C}$  ions), but their beam-delivery system is based on passive shaping techniques. Moreover, NIRS applies multiple beam ports on subsequent days, not on the same day, like GSI. Because the biological repair processes that are relevant for the fractionation effect are mostly completed the next day, the superposition of biologically effective doses is linear on a day-by-day basis. Due to time constraints, this is not an option at GSI. It is the purpose of this paper to present the GSI approach as well as the results obtained so far.

## MATERIALS AND METHODS

All computations are based on our standard radiobiological model<sup>6,7)</sup>, which is an integral part of our treatment planning system, TRiP<sup>1)</sup>. The same software version as that used for patient planning is utilized. Calculations were performed with geometrical setups very similar to those used in clinical practice, but we assumed a spherical target volume of 40 mm in diameter in the center of a spherical water phantom of  $\approx 180$  mm in diameter. Chinese hamster ovary (CHO) cells were used for modelling and verification. Although the cell experiments were performed using rectangular target volumes, it can be assumed that the different target

shapes did not significantly affect the radiation quality. For a comparison between the cell experiments and the calculation, only the line through the isocentre was considered. Two clinically relevant tumours, chordoma and adenoid-cystic carcinoma (ACC), were considered in our model calculations.

The problem can be divided into three parts. First, it has to be verified experimentally by means of *biological dosimetry*<sup>8,9)</sup> that the superposition of two opposing fields yields the expected results. That is, the response of cells, as indicated by a relevant biological endpoint, has to be measured as a function of depth in water and compared with model calculations. This is mandatory in view of the complexity of the biologically effective-dose calculation. Relevant biological endpoints in the context of radiotherapy are the cell survival for tumour tissue and side effects for normal tissue, such as erythema. In this paper only cell survival is considered, since we exclusively deal with dose prescription in the target volume. The term *biological dosimetry* was chosen because of its equivalence to the clinical dosimetry of the absorbed dose distribution in a water phantom. Second, the feasibility of single-port optimization with a subsequent dose overlay has to be demonstrated for both symmetrically and differently weighted partial fields. This is necessary because it cannot be taken for granted a priori that singly optimized fields add to a homogeneous target dose. Third, simple *sum rules* have to be established to account for the nonlinear addition of biologically effective dose levels. Finally, the whole procedure must be practically applicable to patient treatment. In the following section these tasks are discussed step by step.

## RESULTS

Step 1 of our task list is illustrated in Fig. 1. It compares model calculations with experimental results<sup>9)</sup> of the survival of CHO cells irradiated with two symmetric opposing fields of carbon ions. The energies ranged from 160 to 230 MeV/u, corresponding to LET values of between 18.6 and 14.7 keV/ $\mu\text{m}$ . The two partial fields were optimized separately to obtain a constant biologically effective dose of  $\approx 3.8$  Gray Equivalent (GyE). In order to allow for a comparison with photon irradiation, we give the biologically effective dose in GyE, which differs from the absorbed dose (measured in Gy) by the factor RBE. Subsequently, the two fields are overlaid, which implies a new RBE calculation based on the sum of the particle fluences from both sides. The resulting sum dose is  $\approx 6.5$  GyE, corresponding to a 10% survival level. The overall agreement is fairly good; deviations exist mainly in the two entrance channels, where the calculation overestimates the cell killing. This, however, could also be due to systematic experimental errors, and has also been seen in other cell experiments based on stacks (Scholz 1999, private communication). In any case, the calculations are on the safe side for clinical applications, since the damage to the healthy tissue would be overestimated rather than underestimated.

Figure 2 (left hand side) shows step 2 of our task list, that is, partial fields — singly optimized to a given target — add up to a total effective dose distribution which is constant throughout the target region. This can be attributed to an equilibration of the RBE across the

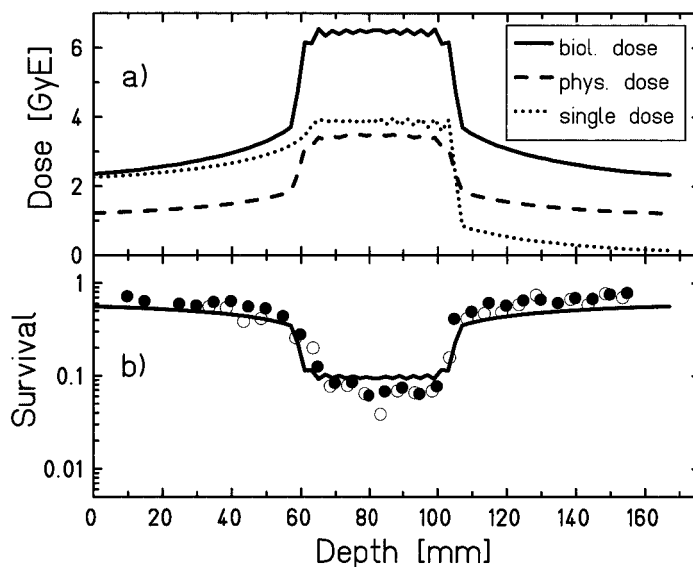


**Fig. 1.** Dose distribution and survival as a function of depth for CHO cells exposed to two opposing fields of carbon ions with energies between 160 and 230 MeV/u. (a) Calculated physical and biologically effective dose profiles. The sum distributions (solid, dashed) as well as the unilateral effective dose profile (dotted) are shown. (b) Measured (symbols) and calculated (lines) survival. The different symbols represent two independent sets of measurements.

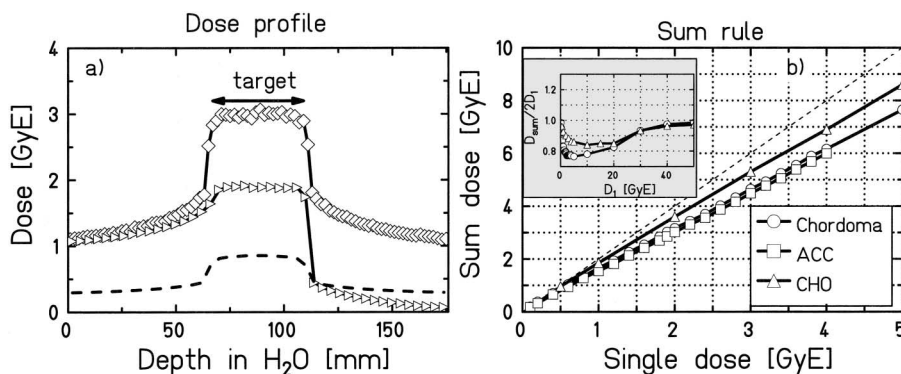


**Fig. 2.** Overlaying of opposing fields with equal weights. Left hand side: Depth profiles of biologically effective dose for chordoma cells,  $\square$ : left partial field (the corresponding field from the right is just the mirror image),  $\triangle$ : sum. The dashed line is the corresponding physical (absorbed) sum dose. Right hand side: Calculated nonlinear sum rule for adding biologically effective doses. The dashed line indicates a linear addition. The inset shows the deviation from linearity as a function of the partial dose level for CHO and chordoma, respectively.

target volume. Regions with smaller RBE in the left field are overlaid with regions of larger RBE in the right field, and vice versa. The resulting absolute biologically effective dose, however, adds up nonlinearly. As an example, we have chosen chordoma cells, because they

represent one of the tumour types most frequently irradiated at GSI. 1.9 GyE is needed in each single field to obtain a total dose of 3 GyE. This can be explained qualitatively by the fact that RBE is dose-dependent. High doses correspond to small RBE, and vice versa. Adding two biologically effective dose values would result in a higher physical total dose value with a smaller RBE in the center of the target volume; hence the biologically effective total dose value would be lower than expected from simple arithmetic.

We now proceed to step 3 of our task list, i.e. establishing sum rules. The right part of Fig. 2 shows the sum rules for the three cell types considered here. Single opposing fields are optimized separately to our standard target volume in order to achieve a homogeneous biologically effective dose distribution. A subsequent superposition of the single fields including a new RBE calculation — based on the sum of the obtained particle fluences from both sides — then yields the biologically effective total dose distribution.

For practical purposes, the partial dose values required to obtain a given sum dose can be read off the graph's x-axis. The small inset graph illustrates the deviation from linearity over a larger dose range, where the ratio  $L = D_{sum} = 2D_1$  is a measure for linearity ( $L = 1$  for perfect linearity).

In clinical practice, asymmetric fields are often applied; that is, the partial fields are applied with different weights. The left part of figure 3 demonstrates that single field optimization can also be applied in such cases, and that a homogeneous dose distributions can be obtained for differently weighted partial fields as well. The sum rule, however, cannot be visualized as a single curve any more, because now two independent variables, the partial doses  $D_1$  and  $D_2$ , must be considered. Instead, a two-dimensional map has to be established where the different partial doses can be read off the coordinate axes for any desired sum dose

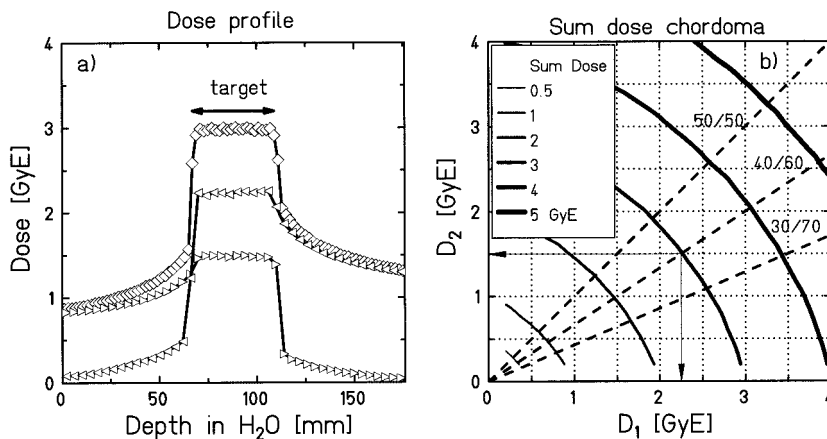


**Fig. 3.** Overlying of opposing fields with asymmetric weights. Left hand side: Depth dose profile,  $\square$ : left partial field,  $\triangle$ : right partial field,  $\diamond$ : sum. Right hand side: Calculated twodimensional map of biologically effective sum dose levels [GyE] as a function of the two partial dose levels. The solid lines are isodose lines; the dashed lines represent dose ratios for different weights. The arrows indicate the single partial dose values to be selected for a resulting dose of 3 GyE and a 40:60 weighting of the two partial fields.

and partial dose weights. Such a map is graphed in the right part of Fig. 3. It was found empirically that the isodose curves can be conveniently parametrized in polar coordinates  $(r, \phi)$  as follows:

$$\begin{aligned} r &= D_{\text{sum}} = ((\cos(\phi))^p + (\sin(\phi))^p), \\ D_1 &= r \cos(\phi), \\ D_2 &= r \sin(\phi), \end{aligned} \quad (1)$$

where  $p$  is an adjustable parameter which depends on the cell type and the sum dose level ( $D_{\text{sum}}$ ). A linear superposition is approached for  $p \rightarrow 1$ , where the isodose curves would become straight lines. For  $p \rightarrow 2$ , the isodose curves would become circles. A least-squares fit of equation 1 to the isodose curves yields the values of  $p$  collected in Table 1 for the cell types under consideration.

The application to a patient plan for a chordoma is shown in Fig. 4. Two symmetric fields with 1.9 GyE each were optimized separately, subsequently overlaid and — based on

**Table 1.** Values of parameters  $p$  in equation 1

Sum dose [GyE]	0.5	1.0	2.0	3.0	4.0	5.0
tissue						
ACC	1.46	1.65	1.81	1.85	1.87	1.87
Chordoma	1.33	1.43	1.61	1.68	1.73	1.76

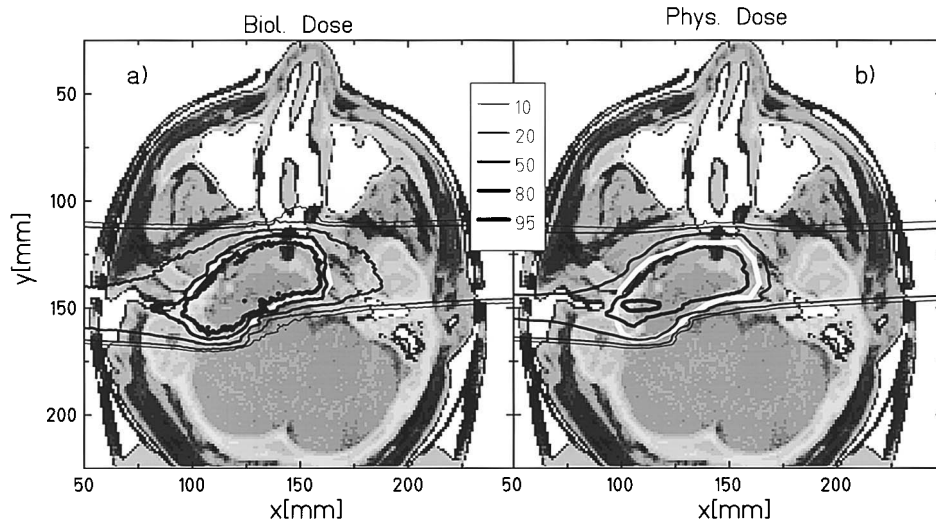


**Fig. 4.** Dose distributions resulting from the overlaying of two opposing symmetric fields for a patient (chordoma). The total prescribed dose was 3.0 GyE. The isodose lines are in percent. The calculation results are graphed on top of a CT image slice through the isocentre. The blank line indicates the target region. (a) biologically effective dose distribution, normalized to 3.0 GyE (100%). (b) corresponding physical dose distribution, normalized to  $\sim 1.0$  Gy (100%).

the accumulated particle fluences — the resulting combined RBE was determined in each voxel, which yielded a biologically effective dose of 3 GyE. The resulting biologically effective dose distribution is essentially flat over the target volume. Both the 85% and the 90% isodose lines conform well to the target contour.

Most of our patients were treated with these or similar field configurations. All biologically effective sum dose distributions showed satisfactory homogeneity across the target region.

## DISCUSSION

Figure 1 demonstrates the validity of our approach by comparing it with experimental data. In view of the experimental difficulties usually encountered in cell-survival experiments, the agreement between measurement and calculation is good. However, the deviations, particularly in the entrance and exit channels, deserve future attention. They might be due to dose-rate effects, since heavy-ion irradiations are time-consuming (compared to X-ray irradiations), and hence the cells in the low-dose regions may find time for repair.

Figure 2 (right part) illustrates the sum rules for the effective dose for equally weighted partial fields. As expected, the linearity ( $L$ ) approaches 1 for  $D \rightarrow 0$  as well as for  $D \rightarrow \infty$ .  $L \approx 1$  can be assumed for partial doses  $> 30$  GyE, which corresponds to the dose value ( $D_{cul}$ ) governing the transition from a linear-quadratic to a linear dose response<sup>6</sup>. Hence, in this high-dose region, where there is no repair process, biologically effective doses can be added linearly. The high-dose region, however, is far beyond our fractionation scheme of 3 GyE given in daily fractions.

Figure 3 presents results for differently weighted fields, which have been used in clinical practice in a number of cases. Equation 1, together with the values collected in table 1, was derived empirically from the numerical results of dose superposition in only the target region. It cannot, at least not with the parameters given in table 1, be applied to the dose “plateau” region in the entrance channels. Its main purpose is to allow a fast decision about how the biologically effective dose must be partitioned in the target region.

All field superpositions discussed in this paper were calculated for only an opposite direction of  $180^\circ$ , since this is our preferred irradiation geometry. Because the GSI facility lacks a gantry, non-planar irradiations are impossible, and hence were not investigated. Due to the very good dose conformation for one or two fields, multi-angular irradiations were not considered either. Although systematic calculations for angles other than  $180^\circ$  should be performed, they are beyond the scope of this paper. Exploratory calculations showed that as long as the angle is not too far off  $180^\circ$  ( $\pm 20^\circ$ ) the sum rules still apply.

Our computations do not make explicit use of an externally supplied “beam quality”, as represented e.g. by the LET. Our radiobiological model, however, takes into account the particle charge and energy distribution at each voxel, and hence correctly reflects the radiobiological properties of the mixed radiation field of carbon ions.

In conclusion, we have reported on a novel technique to support multiport treatment



planning with large-RBE radiation, such as  $^{12}\text{C}$  ions, based on our standard TRiP therapy planning system. Separate optimization of single fields in the beams-eye-view with subsequent overlaying in the CT system was utilized. The nonlinear properties of biologically effective dose superposition could be reduced to relatively simple sum rules well suited for a routine application in the clinical practice in the GSI radiotherapy project as well as in forthcoming ion therapy installations. Since the beginning of therapy in 1997, the treatment of 57 patients has been planned and carried out, most of them with two overlaid fields, as described above.

In the future, smooth field patching techniques will be investigated, which implies the prescription of inhomogeneous dose-weight distributions for the contributing partial fields. This will require fast and automatized biologically effective dose partitioning on a voxel-by-voxel basis. Algorithms like those described here are well suited to meet that requirement. Even simultaneous multiport optimization, which is one of the next steps to be taken, will benefit from the methods presented here, because they offer a fast way to obtain startup values.

### ACKNOWLEDGEMENTS

The author would like to thank Dr. W. Kraft-Weyrather for performing the biological experiments as well as Dr. M. Scholz and Prof. G. Kraft for numerous discussions.

### REFERENCES

1. Jäkel, O., Krämer, M. (1998) Treatment planning for heavy ion irradiation. *Physica Medica* **XIV/1**: 53–62.
2. Han, Z. B., Suzuki, H., Suzuki, F., Suzuki, M., Furusawa, Y., Kato, T., and Ikenaga, M. (1998) Relative biological effectiveness of accelerated heavy ions for induction of morphological transformation in Syrian hamster embryo cells. *J. Radiat. Res.* **39**: 193–201.
3. Aoki, M., Furusawa, Y., and Yamada, T. (2000) LET Dependency of Heavy-ion induced Apoptosis. *J. Radiat. Res.* **41**: 163–175.
4. Pedroni, E., Bacher, R., Blattmann, H., Böhringer, T., Coray, A. et al. (1995) The 200-MeV proton therapy project at the Paul Scherrer Institute: Conceptual design and practical realization. *Med. Phys.* **22**: 37–53.
5. Kanai, T., Endo, M., Minohara, S., Miyahara, N., Koyama-Ito, H., et al. (1999) Biophysical characteristics of HIMAC clinical irradiation system for heavy-ion radiation therapy. *Int. J. Radiat. Oncol. Biol. Phys.* **44**: 201–210.
6. Scholz, M., Kraft, G. (1996) Track structure and the calculation of biological effects of heavy charged particles. *Adv. Space Res.* **18**, 1/2: 5–14.
7. Scholz, M., Kellerer, A. M., Kraft-Weyrather, W., Kraft, G. (1997) Computation of cell survival in heavy ion beams for therapy — the model and its approximation. *Rad. Environ. Biophys.* **36**: 59–66.
8. Mitaroff, A., Kraft-Weyrather, W., Geißl, B., Kraft, G. (1998) Biological verification of heavy ion treatment planning. *Radiat. Environ. Biophys.* **37**: 47–51.
9. Kraft, G., Kraft-Weyrather, W., Taucher-Scholz, G. and Scholz, M. (1997) What kind of radiobiology should be done at a hadrontherapy centre? In: *Advances in Hadrontherapy*, Eds U. Amaldi, B. Larsson and Yves Lemoigne, pp. 38–54, Elsevier, Amsterdam.